Rupture Mechanisms of Elastomer–Metal Adhesive Systems

J. SCHULTZ and N. J. WESTBROOK, *Centre de Recherches sur la Physico-Chimie des Surfaces Solides, C.N.R.S., 68200 Mulhouse, France*

Synopsis

This paper studies the influence of adverse conditions of stress and environment on a conventional industrial two-coat adhesive system for bonding filled elastomers to steel. Several test methods were used in order to produce rupture at the elastomer/adhesive interface, but even the most stringent stress distributions produced *rupture in the elastomer* under relatively rapid constant strain rate testing conditions. However, under fixed strains termed "static fatigue" below immediate rupture conditions, *fracture occurred cohesively in the adhesive.* This fracture originated in the elastomeric phase of the adhesive. Comparison of elastomer and adhesive creep curves show that the locus of failure depends only upon the ultimate properties of the phase in which fracture occurs. This becomes more complicated for propagation of the fracture because of the influence of rheological, thermodynamic, and morphologic aspects of the other constituents of the assembly. *A third type of rupture, produced at the metal surface,* was observed by testing under corrosive conditions such as saline solution. Throughout the study, original observations are confirmed for systems using different elastomers, adhesives, or metal surface coatings.

INTRODUCTION

The adhesion of elastomers to metal, because of its importance, has been the subject of much research, both from a scientific and technologic point of view. Research workers have examined the influence of surface properties using models provoking interfacial failure and, hence, measuring the "real" energy of adhesion. These conclusions are, however, considerably limited in scope because of the use of weak adhesives. Conversely, materials specialists have used industrial systems giving varied fractures classed either by the ultimate joint strength or by the rupture mode. This still does not give a "true" value of the energy of adhesion; the ultimate strength also depends on the mechanical deformation of the adherends, and the rupture mode depends essentially upon the stress distribution in the joint.

Furthermore, although it is possible to predict statistical lifetimes of an adhesive assembly, it is difficult to give an explanation for premature failure of the joint. Being ignorant of the factors determining this lifetime, one is generally incapable of carrying out modifications to lengthen it.

This paper is part of the work[1] undertaken to explain experimental observations and to resolve these problems in a scientific manner. The initial study of rupture phenomena using industrial adhesive systems and conventional adhesion tests was followed by a study of the actual rupture location and the factors influencing a change of location.
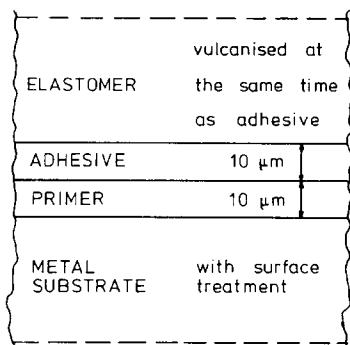
Fig. 1. Cross section of the adhesive assembly.

THE ADHESIVE ASSEMBLY

Although various methods exist for bonding an elastomer to metal, organic polymer adhesives are by far the most common in use today. The problem of finding a compound which has a polarity high enough to adhere to a metal and low enough to adhere to a practically nonpolar elastomer was resolved by using two coats—a polar metal primer P1 and the actual adhesive A1 (Chemlok Type, Hughson Chemical Co, Erie, Pennsylvania, U.S.A.) (Fig. 1).

Little is known about the composition of the adhesives used in this study, except for general indications given by patents[2] and certain publications by Sexsmith[3,4] which state that the constituents are mainly a halogenated polymer probably of an elastomeric nature, a halogenated thermosetting resin, carbon black, specific vulcanizing agents, organic solvents, and small amounts of other materials such as accelerators and reactive salts. The glass transition temperature T_g was determined in the laboratory using a classical dynamic method to locate rapidly the number of phases and the approximate T_g values and a dilatometric method for more precision. These two methods show the existence of two T_g values, one at low temperatures ($T_{g1} = -20°C$) corresponding to the elastomeric phase, the other at high temperatures ($T_{g2} = +95°C$) corresponding to the vitreous phase, in accordance with Sexsmith's indications.

The elastomers were mainly natural rubber (NR) or styrene–butadiene rubber (SBR), 23.5/76.5, although use was also made of nitrile (NBR), chloroprene (CR), butyl (IIR), and ethylene–propylene (EPDM) rubbers to show the influence of the elastomer on the rupture phenomena. The elastomer mixes were of a classical nature containing a reinforcing filler (carbon black), a vulcanizing agent (basically sulfur), accelerators, antioxidants, and plastifiers and were vulcanized so as to obtain an identical hardness. The principal mechanical properties of the elastomers under tension (French Standard NF 46-002 H_2 test piece, rate 20 cm/mn), and the shear (double lap-joint test piece,[1] rate 20 cm/mn) and tear (ASTM D 54 B and C), together with the glass transition temperature, were determined in the laboratory (Table I).

The metal substrate of A-37 mild steel was degreased in trichloroethylene and grit blasted before assembly. Grit blasting increases rugosity and, thus, gives a larger surface area for contact with the adhesive. Two surface treatments, other than the grit blast, were used in order to improve corrosion resistance. These were basically either a galvanization followed by a chromate passivation, or a phosphatization.

TABLE I
Principal Elastomer Characteristics

Elastomer	NR	SBR	NBR	CR	IIR	EPDM
Ultimate tensile strength σ_c, kg/cm^2	210	155	250	190	120	240
Elongation at rupture ϵ_c, %	460	440	640	610	470	530
Modulus at 100% elongation E_{100}, kg/cm^2	25	30	19	17	27	20
Modulus at 300% elongation E_{300}, kg/cm^2	110	120	85	75	85	90
Tear strength ASTMD 624-54(B), kg/cm	100	34	27	29		
Tear strength ASTMD 624-54(C), kg/cm	55	50	54	53		
Shear strength, kg/cm^2	100	105				
T_g, °C	−67	−40				

TABLE II
Results of Three Destructive Tests

	Butt joint	Double lap joint	Peel test
Average joint strength, kg	390	1,100	40
Maximum deviation, %	±17	±10	±10
Bonded			
Area, cm^2	5	10	
Width, cm			2.5
Deformation rate, cm/min	30	30	30

The assembly was prepared by automatically spraying the metal substrate, giving a good reproducibility of thickness (10 μm), with first the primer and then, after drying, the adhesive. Adhesive–elastomer interfacial bonding occured at the same time as vulcanization of the elastomer by injection molding at 155°C and 200 kg/cm^2 pressure for an optimum vulcanization time of the elastomer considered.

RUPTURE IN THE ELASTOMER

Adhesion Tests

One of the main problems in the study of adhesion arises from the choice of an appropriate test at the same time practical, reproducible, and above all capable of giving significant data on the mode and the energy of rupture rather than on the deformation of the adherends. Test methods can be either destructive or nondestructive. The latter are useful as a means of industrial control for detecting voids but are rarely of interest for measuring actual adhesive performance.

Three destructive tests, producing different stress distributions, were chosen for a preliminary analysis: the butt joint, the double lap joint, and the peel test.[5] These joints were tested at ambient temperature and at constant rate of deformation on an Instron testing machine (Table II).
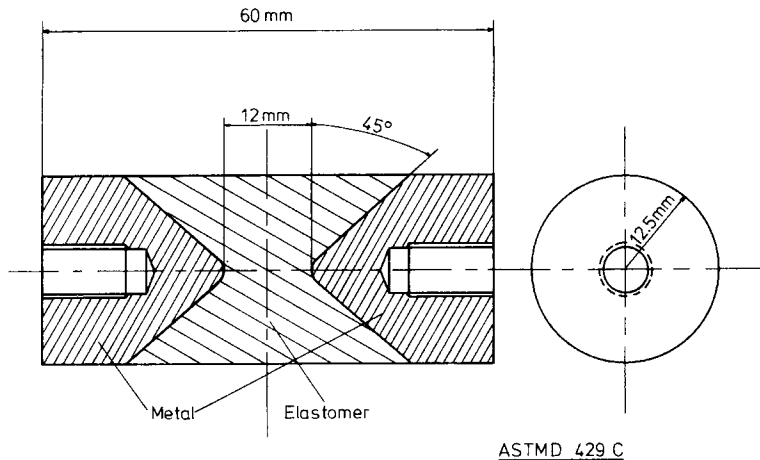
Fig. 2. Painter (bicone)—test piece cross section.

A simple visual examination of the fracture of each joint showed that rupture occurs cohesively in the elastomer (NR). Under these conditions, the results gave no significant information about the adhesion of the constituents of the assembly but simply showed that for the conditions considered, the adhesion was superior to the cohesion of the elastomer.

In order to obtain results relevant to the actual adhesion, a test described by Painter[6] was studied in more detail. The test piece consists of two metal cones bonded together by the elastomeric adherend (Fig. 2).

The interesting point about this testpiece, according to Painter,[6] is the fact that it provokes an interfacial rupture, whereas butt joints or peel tests give cohesive rupture in the elastomer in accordance with the results outlined above. Although adopted by ASTM,[7] the test is relatively underdeveloped, but those authors[8–14] who have adopted it all report a tendency to interfacial failure. These observations led to the present examination.

Figure 3 shows a typical force/elongation curve for the bicone specimen when subjected to constant rate of deformation. Results have shown a precision superior to that obtained with the previous testpieces.

It appears that the conclusions of Painter and others, concerning the mode of rupture of the bicone testpiece, were derived mainly from visual inspection. An attempt to verify their hypothesis was made using thickness measurements and a pyrochromatographic analysis of the layer remaining on the metal cone.

Locus of Failure

Thickness measurements, based on an electromagnetic method, have shown a layer of about 30 μm remaining on the cone after rupture. This value is clearly greater than the sum of the primer and adhesive coats (20 μm). This would seem to indicate that rupture occurs in a zone near to the interface but cohesively in the elastomer.

Immersion of the metal cone in an organic solvent such as benzene after rupture produced a rapid swelling and separation of a thin film. A second film remained on the cone, swelling much less rapidly. From a purely qualitative point
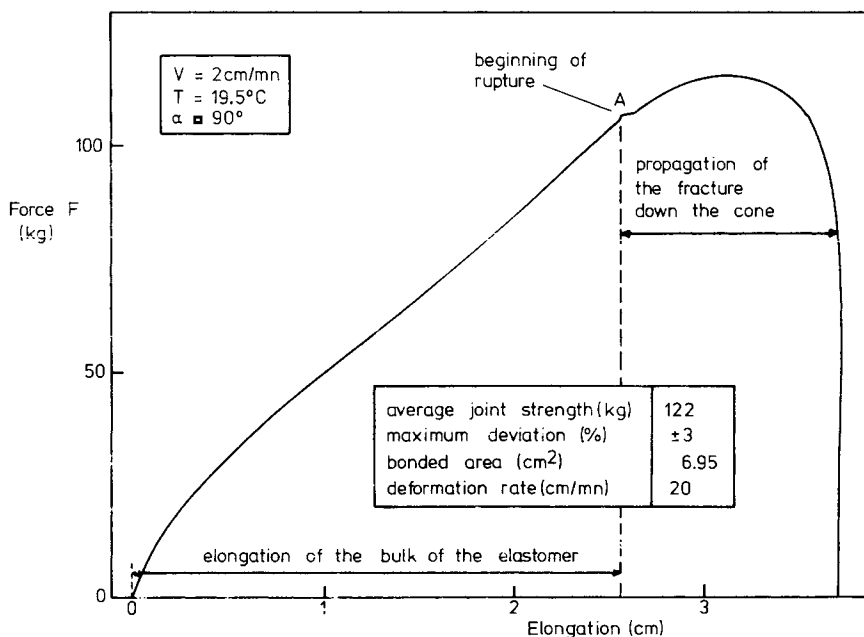
Fig. 3. Typical force–elongation curve for a bicone with cone angle α of 90° and cone tip radius r of 0.8 mm tested at 2 cm/min deformation rate and at ambient temperature.

of view, the swelling of natural rubber and the adhesive in benzene corresponds to that of the two pellicles. These observations were confirmed by comparing the chromatograph obtained after pyrolysis of the detached pellicle with those of the adhesive and elastomer; that of the detached pellicle was identical to that of the elastomer.

The sum of these observations indicates the presence of elastomer on the metal after rupture and, consequently, in these particular experimental conditions, that rupture of the bicone test piece occurs cohesively in the elastomer in a zone near to the elastomer–adhesive interface.

In order to confirm these observations and eventually modify the locus of rupture, a study was undertaken of the influence of the test piece geometry.

Influence of the Test Piece Geometry

The cone tip radius r and the cone angle α are the two most interesting variables in this case, because of the stress concentrations at the cone tip initiating rupture. The distance between the cone tips was kept constant at 12 mm.

It was found that the influence of the tip radius (0.4, 0.8, 1.2, 2.4 mm) on the ultimate joint strength was practically negligible for a radius of less than 1.2 mm (Table III). However, cones with a larger tip radius (2.4 mm) gave higher rupture strengths because of a partial fracture in the mass of the elastomer far from the interfacial zone. For these high radius tips, the maximum stress developed is no longer sufficient to provoke rupture along the cone surface.

The cone angle (75°, 90°, 120°, 180°), using the standard tip radius of 0.8 mm, gave ultimate joint strengths practically the same for angles of 75° and 90° (Table

TABLE III
Effect of the Cone Tip Radius (r) on the Ultimate Joint Strength
at Various Deformation Rates and at Ambient Temperature

Cone tip radius r, mm	Joint strength, kg				
	50[a], cm/min	10, cm/min	2, cm/min	0.5, cm/min	0.05, cm/min
0.4	125		100	91	84
0.8	129	110	105	108	99
1.2	121	114	108	111	96
2.4	149	145	130	125	121

[a] Deformation rate.

TABLE IV
Effect of the Cone Angle (α) on the Ultimate Joint Strength
at Various Deformation Rates and at Ambient Temperature

Cone angle α, degrees	Joint strength, kg				
	50[a], cm/min	10, cm/min	2, cm/min	0.5, cm/min	0.05, cm/min
75	125	102	97	96	
90	129	110	105	108	99
120	160	144	134	112	108
180	206	70	112	200	96

[a] Deformation rate.

IV), whereas an angle of 120° lead to mixed fractures, mainly in the bulk of the elastomer, with higher failure strengths.

Test pieces having flat substrates ($\alpha = 180°$) gave mixed ruptures with highly dispersed ultimate joint strengths apparently independent of the deformation rate. This dispersion probably arose from inaccuracies in centering the joint, hence accentuating the high shear stresses formed on the outer metal–elastomer edge.

In general, an increase in the cone angle gave a higher probability of rupture in the mass of the elastomer, with a corresponding decrease in precision. Both the tip radius and the angle experiments showed fractures always in the elastomer, but either near the interface or in the bulk of the elastomer according to the test piece geometry. However, the preceding conclusions apply to a metal–primer–adhesive–NR system only.

Influence of the System Constituents

In the case of the metal–adhesive and elastomer–adhesive adhesion remaining greater than the cohesion of the elastomer, a change of metal substrate or adhesive should give no modification of the ultimate joint strength. This hypothesis was confirmed (Fig. 4) for the metal substrate by using galvanized or phosphated metal substrates instead of the original grit-blasted surface denoted by Zn, Ph, or G, respectively. The ultimate joint strength, as a function of the deformation rate, was independent of the metal substrate surface treatment.

Assemblies using two other adhesives (A_2 and A_3) having similar properties to the basic adhesive (A_1) and also used for elastomer–metal bonding not only
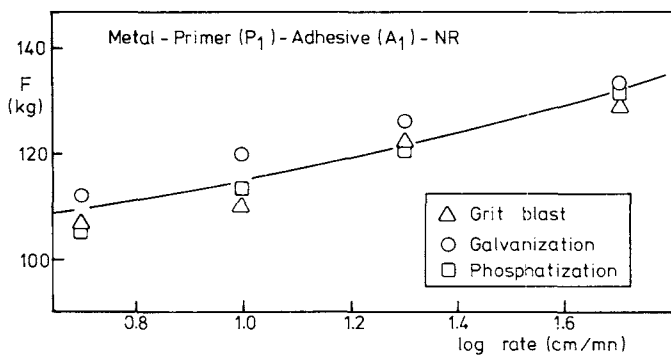
Fig. 4. Influence of change of metallic substrate surface treatment on the ultimate joint strength at various deformation rates and at ambient temperature.
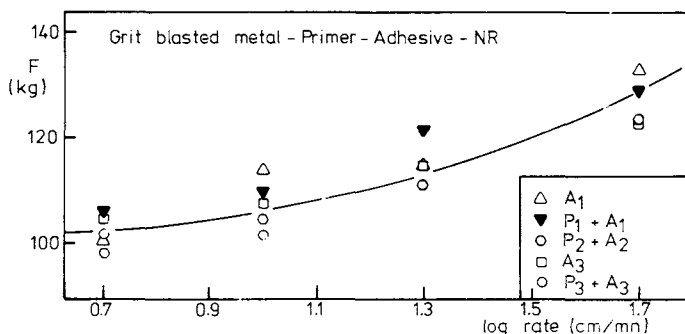

Fig. 5. Influence of change of adhesive on the ultimate joint strength at various deformation rates and at ambient temperature.

showed that the assembly was unaffected by a change of adhesive (Fig. 5), but also that the primer (P_1, P_2, or P_3) had no influence under these conditions.

One can expect the nature of the elastomeric adherent to influence the fracture of the assembly since rupture occurs in the elastomer and large strains are involved.

Ultimate joint strengths and elongations were measured for assemblies made up of SBR, CR, NBR, IIR, or EPDM elastomers (grit-blasted metal–P_1–A_1–elastomer system) (Table V) and compared with ultimate tensile properties of the elastomers. As the elastomer properties are similar (Table I), one would also expect joint strengths to be similar. This is true for all the systems studied with the exception of that using SBR, which gave a much higher joint strength. In addition, the fracture profile is totally different to all the other systems; the fracture no longer propagates down the sides of the cone but in the bulk of the elastomer, perpendicular to the axis of the cone. This difference of fracture mode, important from a practical point of view, is easily explained by considering the elastomer properties in tension and shear together with the cone angle.[1]

Under the conditions examined so far, the ultimate strength of a joint depends neither on the nature of the adhesive nor on the metal substrate treatment but solely upon the mechanical characteristics of the elastomer. The rupture mode (in tension or shear) depends on these characteristics together with the test piece geometry.

TABLE V
Influence of a Change of Elastomer on the Ultimate Joint Strength
Compared with Ultimate Tensile Properties of the Elastomers

	NR	SBR	NBR	CR	EPDM	IIR
Bicone test piece properties at rupture (cross-head speed 20 cm/min)						
Rupture force, kg	117	270	150	100	138	150
Elongation at rupture, cm	2.5	4.1	4.0	3.0	3.9	3.3
Elastomer ultimate tensile properties (cross-head speed 20 cm/min)						
Rupture stress, kg/cm^2	210	155	250	190	240	120
Elongation at rupture, %	460	440	610	640	530	470

As rupture always occurs cohesively in the elastomer, this would suggest a totally adequate adhesive, the adhesion at each interface being superior to the elastomer cohesion. However, the main problem in adhesion is not the difficulty of bonding one solid to another but the fact that adhesion evolves with time, either because of modifications of the interface (corrosion, migration, diffusion) or changes in the properties of the system constituents (aging, fatigue). In fact, when a test piece is submitted to a deformation less than that necessary for cohesive rupture and maintained under stress at constant temperature and strain, rupture occurs after a given time depending upon the applied stress. This type of rupture will be termed "rupture in static fatigue."

RUPTURE IN THE ADHESIVE

Rupture Initiation in Static Fatigue

Test Method

Preliminary studies showed that for an SBR bicone test piece, this second type of fracture propagates along the cone instead of in the bulk of the elastomer as observed for constant deformation rate testing. Thickness measurements, confirmed by solvent swelling, showed the existence of a film 15 μm thick remaining on the cone after rupture. As the primer and adhesive layers together were approximately 20 μm thick, it would appear that rupture occurred cohesively in the adhesive. Hence, static fatigue changes fundamentally the behavior of the assembly, giving a different locus of failure.

The test piece (the same dimensions as the bicone but with one cone and one flat metal endpiece to avoid simultaneous fracture at both metal–elastomer interfaces), using a grit-blasted metal–primer–P_1–adhesive A_1–SBR system, was held in a metal frame at a given elongation and temperature. After a certain time, the test piece was released, cooled to ambient temperature, and then broken. Fracture in static fatigue propagates along the cone and could easily be distinguished from fracture in the mass of the elastomer. The surface detached, plotted as a function of time, can be extrapolated to zero surface, giving the time necessary for initiation of rupture, τ_T.

Influence of Temperature on Initiation

Relaxation curves of NR and SBR assemblies show that the applied stress at rupture is practically constant; and hence, in the case being examined, i.e., at a constant strain of 2 cm, time and temperature are the only two variables. The variation of τ with temperature is more easily expressed on a logarithmic time scale which would suggest a rheological phenomenon of a viscoelastic nature applicable to the Williams, Landel, and Ferry relation.[15] This can be written here as

$$\log \frac{\tau_T}{\tau_{T_S}} = \log a_T = \frac{C_1(T - T_S)}{C_2 + T - T_S}$$

where τ_T and τ_{T_S} are the times necessary to initiate rupture at a temperature T and a reference temperature T_S, respectively; a_T is the shift factor relating τ_T to τ_{T_S}; and C_1 and C_2 are constants.

A linear relationship between $(T - T_S)/(\log \tau_T/\tau_{T_S})$ and $(T - T_S)$ shows that the WLF equation is applicable and that a viscoelastic phenomenon is the origin of static fatigue. The experimental points (Fig. 6) correspond well with the theoretical WLF curve calculated for T_g of $-20°C$.

It can thus be concluded that the viscoelastic phenomenon of static fatigue has as its origin the elastomeric phase of the adhesive.

Influence of the System Constituents

When rupture in static fatigue occurs in the adhesive, the initiation period should depend only upon the nature of the adhesive. This was confirmed for the elastomer using identical tests on an NR-based test piece (Fig. 6) and for the metal surface using grit-blasted (G), phosphatized (Ph), or galvanized (Zn) surfaces with or without a primer coat.

However, as expected, test pieces using different adhesives (A_1, A_2, or A_3) gave different initiation times; and at 80°C and 2 cm elongation, the test pieces using the adhesives A_2 and A_3 gave a resistance to fatigue approximately five times greater than those based on the adhesive A_1 under these particular experimental conditions.

Mechanism of Static Fatigue

Two mechanisms can be envisaged for the initiation of rupture in a viscoelastic solid: (a) if it is not crosslinked, a disentanglement and sliding of the macromolecular chains (corresponding to adhesive A_3); and (b) if it is crosslinked, the growth of a flaw up to a critical size (corresponding to adhesive A_1).

In the case of an elastomer–adhesive assembly, the stress in either component can be considered equal near the interfacial zone, and creep will occur until the critical rupture time is reached for one of the components, either the adhesive or the elastomer. The rupture curves for dumbbell specimens, in tensile creep, of SBR and adhesive A_1, (Fig. 7) show that at 20°C, rupture of the assembly will occur for a low applied stress in the adhesive and, for a higher applied stress, in the elastomer. At a higher temperature of 80°C, the two curves no longer cross, in the range of stress considered, and the rupture curve of the assembly is entirely
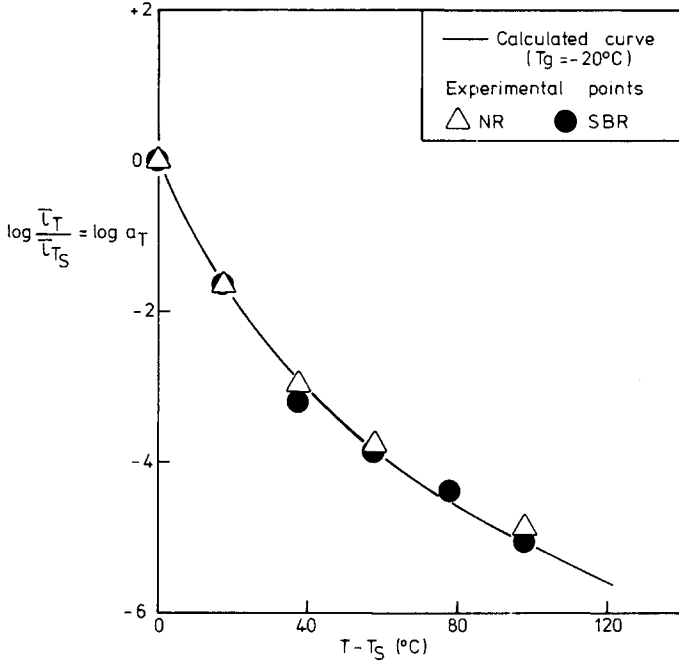
Fig. 6. Influence of change of elastomer on the initiation period τ_T. Comparison of the experimental results to the theoretical WLF curve calculated for $T_g = -20°C$ ($T_S = 22°C$).
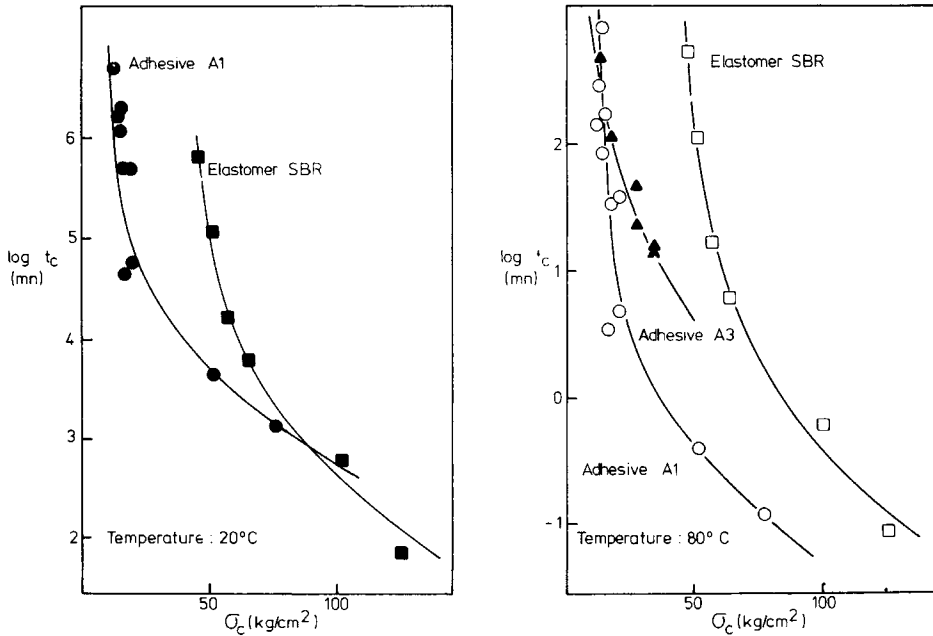

Fig. 7. Rupture curves (time to rupture t_C as a function of stress at rupture σ_C) obtained from tensile creep curves of SBR and adhesives A_1 and A_3 at 20° and 80°C.

determined by the adhesive. In addition, the adhesive A_3 is superior to A_1 under these conditions.

These results show how, knowing certain rheological characteristics, one can predict the fracture mode (in the adhesive or in the elastomer) of an assembly under tensile creep. These considerations can, most probably, be applied to assemblies under different conditions of stress, uniaxial or multiaxial, static or dynamic, and other forms of test (creep, relaxation, constant rate deformation, etc.). This hypothesis is justified by the results obtained with the bicone test piece. This test piece, developing multiaxial stresses at constant deformation rate, gave ruptures in the elastomer at high applied stresses and short times. However, in static fatigue, at much lower applied stresses, rupture occurred in the adhesive after a much longer time interval. This test has also shown the superiority of the adhesive A_3 at 80°C. Hence, the initiation of rupture in static fatigue depends only upon the rheological properties of the adhesive. The propagation of fracture is a different problem.

Fracture Propagation in Static Fatigue

Test Method

In order to follow the displacement of the rupture front, a 90° peel test[5] proved to be more appropriate than the bicone test piece. Electron microscopy confirmed that the fracture, as well as originating, continued to propagate within the adhesive. However, the peel energy measured results mainly from elastomer deformation. The constituents of the system can now be expected to have some effect on the fracture propagation, and their influence was examined by measuring peel energy as a function of the rate of propagation and temperature.

Influence of System Constituents

Assemblies based on NR and SBR showed that, for a given rate of separation, the peel energy for the NR system was greater than that of the SBR even though rupture occurred in the adhesive. Following the reasoning of Gent and Schultz,[16] extended to cohesive failure by Andrews,[17] this difference is due to energy dissipated in the viscoelastic solid which can be related, at least qualitatively, to the energy dissipated during dynamic deformation. Determination of the loss modulus E'' (Fig. 8) confirmed that $E''_{NR} > E''_{SBR}$ for the temperatures used in the peel tests, i.e., higher than 100°C, and, hence, that the peel energy of systems differing only by their elastomer is governed by the dissipation of energy within the mass of the elastomer. It is also interesting to note that an elastomer which has a good resistance to peeling at ambient temperatures can become relatively weak at higher temperatures.

Since rupture occurs in the adhesive, it is to be expected that a change of adhesive will give rise to a different peel energy. For assemblies differing only by the adhesive, the energy dissipation within the elastomer does not change (at a given peel rate) from one assembly to another, and the ratio of peel energies remains constant independent of the peel rate (Fig. 9). This ratio shows the influence of the reversible cohesive energy of the adhesive on the total strength of the assembly.[16,17]
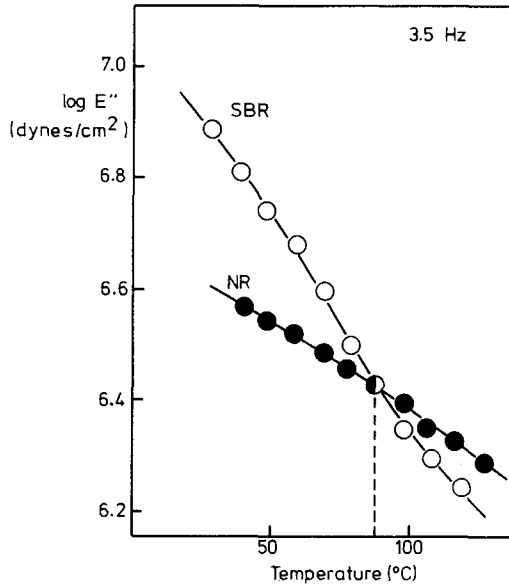
Fig. 8. Loss modulus E'' as a function of temperature for elastomers NR and SBR.
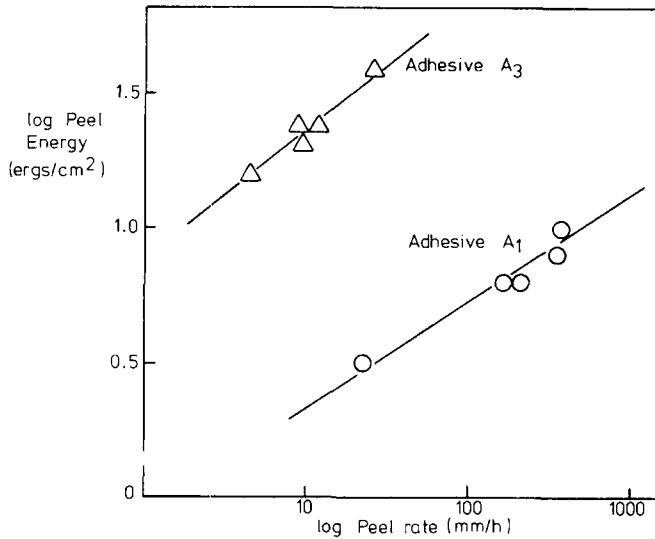

Fig. 9. Influence of change of adhesive on peel energy in static fatigue.

For assemblies differing only by their metal substrate surface treatment, the galvanized and phosphated substrates produced similar results (Fig. 10), whereas the grit-blasted surface gave rise to substantially greater peel energies. However, the rupture propagated within the adhesive in all three cases, the initiation periods were identical, and the metal was undeformed. The difference must, therefore, arise from a difference in the actual surface texture. This was confirmed by microscopy, followed by rugosity measurements, of the maximum depth R_T and the average depth R_A of the surface irregularities (Table VI).
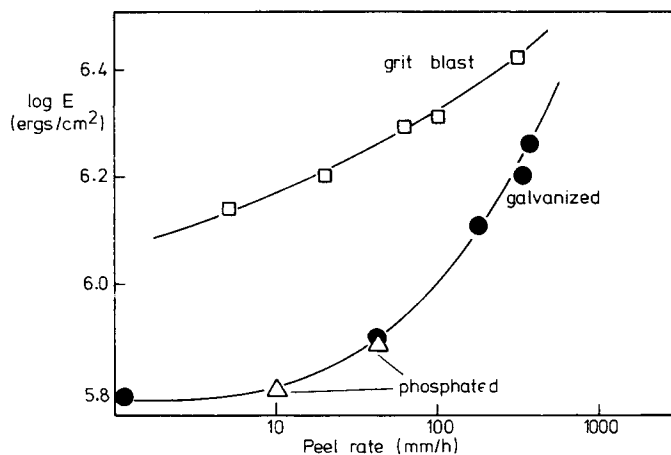
Fig. 10. Influence of change of metal substrate surface treatment on fracture propagation.

The surface after rupture had the same profile as that of the initial metal surface, and, consequently, fracture propagates in the adhesive following the surface contours. Whereas only the rheological characteristics of the adhesive intervene in the case of rupture initiation in static fatigue, the actual propagation of the fracture is governed by the characteristics of all the constituents of the system and can be rheological, thermodynamic, or morphologic.

Finally, under certain conditions, rupture could be observed at the metal substrate when the assembly was submitted to corrosive liquids such as saturated saline solution, a situation likely to be encountered by the assembly during its normal lifetime.

These test were effected by immersing the system in the saline solution at 90°C and varying the peel rates by applying different loads.

RUPTURE AT THE METAL SURFACE

The primer in its role as metal surface protector can now be expected to have an important influence on the assembly (Fig. 11).

Behavior Without Primer

These assemblies produced, throughout the whole range of peel rates, a rupture at the metal surface. This is due to a corrosion of the metal during peeling, a

TABLE VI
Rugosity of the Metal Substrate, Initially and After Rupture
(Maximum Depth R_T and Average Depth R_A of Asperities)

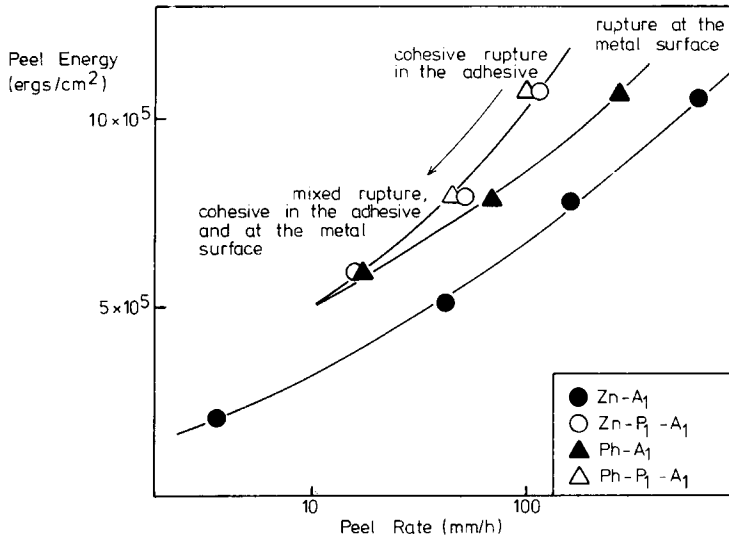| Metal substrate surface treatment	Initial metal substrate		Substrate after rupture	
	R_T, μm	R_A, μm	R_T, μm	R_A, μm
Grit blast	27	7–8	27	5
Galvanization	7–9	2	11–15	2–3
Phosphatization	8–10	2	8–10	2

Fig. 11. Influence of metal substrate surface treatment on fracture propagation (saturated saline solution at 90°C).

conclusion supported by the fact that there is no longer an initiation period before the beginning of peeling. The difference between the two assemblies in Figure 11 is simply due to the different corrosion rates of the phosphated or galvanized metal substrate.

Behavior with Primer

For assemblies having a primer, a phenomenon of rupture occurred (cohesively within the adhesive) at high peel rates, analogous to that in air.

At lower peel rates, corrosion began to intervene giving mixed ruptures (partially within the adhesive, partially at the metal surface). It is probable that at very low peel rates, rupture becomes identical to that of an assembly having no primer.

CONCLUSIONS

This general study of the rupture phenomenon of adhesive elastomer–metal assemblies has shown the different forms of rupture which can be produced according to the type and level of stresses imposed, the characteristics of the system constituents, and the nature of the surrounding environment.

A study of this nature should give rise to practical applications, in particular to an assembly having optimum performance. There can be no general solution to this problem, given the multiplicity of relevant criteria (stress, strain, ultimate strength, resistance to heat and corrosion, etc.) and the complexity of the stress history undergone by the assembly. However, the results presented here should be able to suggest constructive ideas for the improvement of an adhesive assembly under given conditions.

References

1. N. J. Westbrook, Doctorat d'Université, Presented March 21, 1975 Université Louis Pasteur, Strasbourg France.

2. L. A. Brooks, U.S. Pat. 2,637,651 (May 5, 1953). E. W. Coleman and D. M. Alstadt, U.S. Pat. 2,900,292 (August 18, 1959).

3. F. H. Sexsmith, *Adhesives Age,* **13,**(6), 31 (1970).

4. F. H. Sexsmith and R. D. Sites, *Proc. Int. Rubber Conf., Paris,* **3,** 53 (1970).

5. ASTM D 429-64 Method B.

6. G. W. Painter, *Rubber Age,* **86**(2), 262 (1959); *Adhesives Age,* **3**(2), 36 (1960).

7. ASTM D 429-64 Method C.

8. E. Hundertmark, *Plaste Kautschuk,* **13**(10), 593 (1966).

9. D. R. Cox, *Rubber J.,* **151**(4), 49 (1969); *ibid.,* **151**(5), 73 (1969); *ibid.,* **151**(6), 36 (1969).

10. S. L. Brams, *Rubber World,* **142**(4), 67 (1960).

11. J. W. Gallagher, *Rubber World,* **14** (6), 75 (1961).

12. E. Weatherstone, *Rubber J.,* **148**(5), 31 (1966); *Aust. Plast. Rubber J.,* (June 20, 1966); *Plastics Paint Rubber,* 63 (Jan./Feb. 1967); *ibid.,* 77 (Mar./Apr. 1967).

13. B. Pickup and E. Weatherstone, *J. IRI,* **3**(6), 254 (1969); *Ind. d. Gomma,* **13**(4), 42 (1969).

14. W. De Crease, *Rubber Age,* **87,** (6), 1013 (1960).

15. M. L. Williams, R. F. Landel, and J. D. Ferry, *J. Amer. Chem. Soc.,* **77,** 3701 (1955).

16. A. N. Gent and J. Schultz, *Proc. Int. Rubber Conf.,* Brighton **C1,** 1 (1972).

17. E. H. Andrews and A. J. Kinloch, *Proc. R. Soc.* London, **332,** 401 (1973).